

An Efficient and Reliable Asynchronous Federated Learning Scheme for Smart Public Transportation

Chenhao Xu, Youyang Qu, *Member, IEEE*, Tom H. Luan, *Senior Member, IEEE*, Peter W. Eklund, Yong Xiang, *Senior Member, IEEE*, and Longxiang Gao, *Senior Member, IEEE*

Abstract—Since the traffic conditions change over time, machine learning models that predict traffic flows must be updated continuously and efficiently in smart public transportation. Federated learning (FL) is a distributed machine learning scheme that allows buses to receive model updates without waiting for model training on the cloud. However, FL is vulnerable to poisoning or DDoS attacks since buses travel in public. Some work introduces blockchain to improve reliability, but the additional latency from the consensus process reduces the efficiency of FL. Asynchronous Federated Learning (AFL) is a scheme that reduces the latency of aggregation to improve efficiency, but the learning performance is unstable due to unreasonably weighted local models. To address the above challenges, this paper offers a blockchain-based asynchronous federated learning scheme with a dynamic scaling factor (DBAFL). Specifically, the novel committee-based consensus algorithm for blockchain improves reliability at the lowest possible cost of time. Meanwhile, the devised dynamic scaling factor allows AFL to assign reasonable weights to stale local models. Extensive experiments conducted on heterogeneous devices validate outperformed learning performance, efficiency, and reliability of DBAFL.

Index Terms—Asynchronous Federated Learning, Blockchain, Dynamic Scaling Factor, IoV.

I. INTRODUCTION

MACHINE learning (ML) is a popular approach on the Internet of Vehicles (IoV) to enable smart public transportation [1], [2]. For example, buses with ML models are able to forecast traffic flows and the time passengers wait at stops, assisting drivers in improving driving safety and fuel economy. However, because traffic conditions change over time, ML models must be updated continuously and efficiently. Federated Learning (FL) is a distributed ML scheme that allows models to be trained locally and updated frequently. For instance, buses collect traffic data and train local models, while roadside units (RSUs) periodically aggregate the local models to produce an accurate global model and send it back to the buses [3].

However, FL raises efficiency and reliability concerns due to the limited computing resources and continuous movement of

buses in smart public transportation. Firstly, the synchronous aggregation strategy forces the aggregation server to collect enough local models before aggregation, which is inefficient due to the difference of computing power and dataset sizes among buses and RSUs [4]. Specifically, high-performance nodes have to wait for lagging nodes to finish their training before aggregation. Secondly, unreliable local models gathered from buses pose FL at risk of poisoning attacks [5]. The centralized aggregation server of FL is subject to DDoS attacks [1]. Both of these attacks reduce the reliability of FL.

To improve the efficiency of FL, asynchronous federated learning (AFL) is proposed, which reduces the latency by performing aggregation whenever a local model is received [6]–[10]. However, due to the high aggregation frequency, there are outdated global models in AFL, from which stale local models trained usually have relatively low accuracy [11]. Existing work either discards or assigns irrational weights to stale local models, leading to unstable FL learning performance (i.e. convergence speed and global model accuracy) [4].

Some work adopts blockchain to improve the reliability of FL [12]. Due to its decentralized storage, attack-proof consensus algorithm, and self-verifying smart contracts [13], [14], blockchain allows FL to conduct a decentralized and transparent training process, resulting in improved security and trustability. However, consensus algorithms of the blockchain are either compute-intensive (i.g. PoW) or communication-intensive (i.g. PBFT) [4]. To improve efficiency, committee-based consensus algorithms such as DPoS are proposed [15], but their token or reputation systems are unsuitable for buses that pass quickly. Although several blockchain-based AFL schemes are proposed [16]–[18], their consensus processes are still time-consuming.

In order to address the above challenges and better apply FL into smart public transportation systems, this paper offers a blockchain-based asynchronous federated learning framework with a dynamic scaling factor (DBAFL). A novel committee-based consensus algorithm is introduced to improve reliability while bringing the least amount of communication burden. Specifically, the committee leader, as the aggregation server, identifies low-accuracy local models based on its local dataset to resist poisoning attacks. Without the need for communication and voting, a new committee leader is elected from RSUs periodically based on the hash of the latest block to reduce the risk of being subjected to DDoS attacks. Besides, when performing aggregation, a dynamic scaling factor is designed to assign appropriate weights to local models according to their accuracy and correspondingly improves the learning

Longxiang Gao is the corresponding author.

Chenhao Xu and Yong Xiang are with the Deakin Blockchain Innovation Lab, School of Information Technology, Deakin University, Geelong, Australia. E-mail: {xueri and yong.xiang}@deakin.edu.au.

Youyang Qu is with Data 61 Australia Commonwealth Scientific and Industrial Research Organization, Australia. E-mail: youyang.qu@data61.csiro.au.

Tom H. Luan is with School of Cyber Engineering, Xidian University, Shaanxi, China. E-mail: tom.luan@xidian.edu.cn.

Peter W. Eklund is with School of Information Technology, Deakin University, Geelong, Australia. E-mail: peter eklund@deakin.edu.au.

Longxiang Gao is with Qilu University of Technology and Shandong Computer Science Center, China. E-mail: gaolx@sdas.org.

performance of FL. Experiments conducted on heterogeneous devices evaluate the proposed scheme and demonstrate its outstanding learning performance, efficiency, and reliability. The main contributions of this paper are as follows.

- A blockchain-based asynchronous federated learning scheme is designed for smart public transportation, considering learning performance, efficiency, and reliability in heterogeneous computing environments.
- A dynamic scaling factor is designed to assign appropriate weights to stale local models with the joint effort of a committee-based consensus algorithm, allowing FL to efficiently converge to higher accuracy while being highly attack-resistant.
- An open-source prototype¹ is implemented with comprehensive experiments conducted to validate the advantages from three perspectives compared with state-of-the-art schemes.

The remainder of this paper is organized as follows: Section II presents related work. Section III models the proposed scheme in detail. Section IV analyzes the proposed scheme from several aspects. Section V evaluates the proposed scheme experimentally. Finally, Section VI summarizes the paper and outlines future work.

II. RELATED WORK

The related work of this paper includes the blockchain, federated learning, IoV, and asynchronous federated learning.

A. Blockchain, Federated Learning, and IoV

Some existing work integrates the blockchain and FL to resist attack in classic FL [1], [13], [16]–[26]. The blockchain is a motivation for the nodes to participate in FL and contribute high-quality local models [19], [20], [27], a distributed reputation management system to resist repudiation and tampering [26], and an auditable distributed database that allows FL to conduct a transparent training process [21]. However, none of these schemes simultaneously take efficiency and reliability into account. Shayan *et al.* [22] prove that the blockchain effectively defends FL against poisoning attacks. Li *et al.* [23] design a committee consensus algorithm for blockchain-based FL without analyzing the communication burden brought by the blockchain. Besides, the score-based committee election in their scheme is unsuitable for fast-traveling buses. Kang *et al.* [28] propose a hierarchical blockchain-based FL scheme with improved efficiency and privacy, but miner election and model quality cross-validation in the consensus process are time-consuming and inappropriate for buses.

There are some work adopts FL in IoV. For example, Lim *et al.* [29] propose a blockchain-based IoV network that matches the lowest cost Unmanned Aerial Vehicles (UAVs) to each subregion, but communication latency is not analyzed and tested. Besides, some work utilizes the blockchain to ensure a secure FL framework on IoV networks, including data sharing [24], driving assistance [30], and intrusion detection [31]. However, these schemes are inefficient on IoV networks due

to the synchronous aggregation strategy. Pokhrel *et al.* [25] optimize the latency by adjusting the block arrival rate, but the PoW consensus in their scheme is still time-consuming. Lu *et al.* [1] introduce the directed acyclic graph architecture to the blockchain to improve efficiency, but security and communication latency are not analyzed.

DBAFL introduces a novel committee-based consensus algorithm to the blockchain, which brings the least communication latency to buses while ensuring reliability.

B. Asynchronous Federated Learning

FL, proposed in 2017 [3], is a distributed learning scheme applied in various scenarios [32]–[35]. To reduce aggregation latency and improve efficiency on resource-limited networks, AFL is proposed [6]–[10], [16].

A semi-asynchronous FL scheme is proposed for mitigating model staleness [8]. However, lagging models in their scheme are given the same weight as normal models during aggregation. Chen *et al.* [6] assign a higher weight to stale local models due to large training datasets. But stale local models in IoV networks may be due to inadequate computing power. Chen *et al.* [7] improve efficiency by reducing the updating frequency of parameters in deep layers, which is hard to apply to other types of models. Liu *et al.* [16] propose an AFL framework with a staleness coefficient to adjust the weight of stale local models, but analysis and validation are missing. Lu *et al.* [9] present a new gradient compression approach to improve efficiency at the cost of global model accuracy. Deng *et al.* [10] propose a semi-AFL approach APFL that mixes the parameters of local and global models to lower communication frequency, but an additional training phase is required. Chen *et al.* [30] present a blockchain-based AFL scheme BDFL with all models saved in the blockchain and aggregated with the same weight. As highly relevant work, APFL and BDFL are included as benchmarks in Section V.

A dynamic scaling factor is designed in DBAFL for weighted aggregation according to model accuracy, which improves learning performance and reliability.

III. DBAFL MODELING

This section explains the model of DBAFL in detail from the aspect of the system model, workflow, dynamic scaling factor, and committee-based consensus algorithm.

A. System Model

The public transportation system includes buses and RSUs on a road, as shown in Fig. 1. The bus stop equipped with sensors and an edge computing server is considered a kind of RSU in this scenario. RSUs usually have higher computing and communication power than buses. Buses establish short-term Vehicle-to-RSU (V2R) and Vehicle-to-Vehicle (V2V) connections with nearby RSUs or buses when they are within a signal region, allowing them to transmit a certain amount of data. Besides, RSUs have a high-speed Ethernet connection with each other to support smart public transportation.

Buses and RSUs train ML models collaboratively to predict traffic flows and the time passengers wait at stops,

¹The Github link is <https://github.com/xuchenhao001/AFL>.

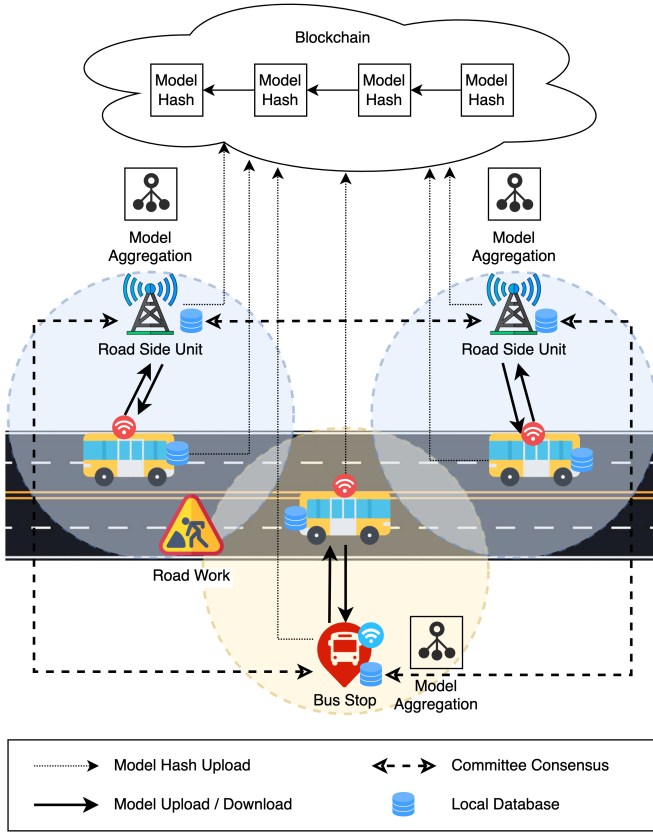


Fig. 1. The architecture of DBAFL in public transportation.

allowing buses to travel safely and efficiently. Since traffic conditions change over time, buses and RSUs continuously collect training dataset through their sensors to update models. In an area, buses and RSUs usually observe similar traffic conditions and collect independent and identically distributed (IID) data. However, the training time and model quality of buses and RSUs differ due to differences in computing power and dataset sizes, posing learning performance challenges to FL. The limited connect time and bandwidth of V2R and V2V connections pose efficiency challenges to FL. The poisoning and DDoS attacks launched by attackers on the roadside pose reliability challenges to FL.

In DBAFL, a dynamic scaling factor and a lightweight consensus algorithm are designed on top of AFL and the blockchain to improve learning performance, efficiency, and reliability. Specifically, buses and RSUs act as local nodes of FL and train local models based on their local data. After training, local nodes upload the hash value of the local model to the blockchain for other nodes to verify. Apart from that, buses upload the local model to nearby RSUs for global model aggregation. During the aggregation, the dynamic scaling factor assigns weights to local models according to their accuracy. RSUs are committee members and are eligible to be elected as the committee leader by the consensus algorithm. The identity of the next committee leader is determined by the hash of the most recent block, which does not require voting or communication. The committee

maintains a distributed database with data synchronization to share models. The committee leader is in charge of performing aggregation whenever a new local model is received.

B. Workflow

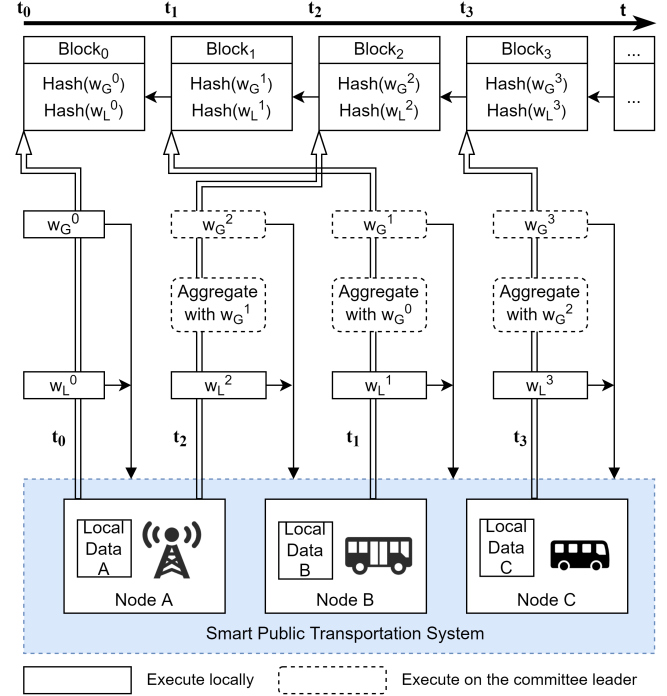


Fig. 2. The workflow of DBAFL.

The workflow of DBAFL is illustrated in Fig. 2. In a smart public transportation system, assume three nodes (Node A, B, and C) are involved in the training process. Specifically, Node A is an RSU, while Node B and Node C are buses. With the passage of time (from t_0 to t_3), the nodes keep training local models with the latest global model. The details are as follows:

At t_0 , Node A trains a local model w_L^0 as the initial global model w_G^0 . Then Node A uploads the hash values of them, i.e. $\text{Hash}(w_G^0)$ and $\text{Hash}(w_L^0)$, to the blockchain to build up a genesis block Block_0 (The first block in the blockchain). After receiving the hash value of Block_0 , each node downloads w_G^0 from Node A, and trains local models based on its local data. At the same time, a committee leader is elected based on the hash value of Block_0 .

At t_1 , Node B finishes its training and generates a new local model w_L^1 . Next, Node B calculates the hash value $\text{Hash}(w_L^1)$ and uploads it to the blockchain. Besides, Node B uploads w_L^1 to the nearby RSU, where it will be stored in the distributed database and shared with the committee leader. Without waiting for other nodes, the committee leader aggregates w_G^0 and w_L^1 according to a dynamic scaling factor, which is explained in Section III-C, to produce a new global model w_G^1 . The committee leader then uploads $\text{Hash}(w_G^1)$ to the blockchain, where a new block Block_1 is generated. The global model w_G^1 is then shared with all committee members.

At t_2 , Node A finishes training based on w_G^0 and acquires a stale local model w_L^2 . Node A uploads $\text{Hash}(w_L^2)$ to the blockchain, along with w_L^2 shared with the committee leader through the distributed database. Based on w_G^1 and w_L^2 , the committee leader generates a new global model w_G^2 , along with the hash value $\text{Hash}(w_G^2)$ uploaded to the blockchain. After that, Block_2 is created and appended to the blockchain.

After a long period of training, Node C finally finishes training its local model w_L^3 based on w_G^0 . Although it is stale, the local model w_L^3 uploaded by Node C is also acceptable for the committee leader. Node C uploads $\text{Hash}(w_L^3)$ to the blockchain at the same time. After aggregating w_L^3 and w_G^2 , the committee leader generates a new global model w_G^3 , and uploads $\text{Hash}(w_G^3)$ to the blockchain. Then, Block_3 is generated.

With the help of blockchain, the training process is consistent, transparent, and trustable. Besides, the novel committee-based consensus algorithm in the blockchain enables an attack-resistant DBAFL with a generalized ML model. The advantages of DBAFL are explained carefully in Section IV-B.

C. Dynamic Scaling Factor

In [6], [7], [16], the authors demonstrate that the weight of local models during aggregation has a significant impact on federated learning performance. If a stale local model has low accuracy due to the limited computing resources of the node, relying too much on this particular local model results in a deterioration of global model accuracy. On the contrary, if the stale local model has relatively high accuracy due to large volumes of data on the node, it is preferential to make better use of it to improve the convergence speed of the global model.

A dynamic scaling factor, denoted as ϵ , is designed to assign the newly arrived local model appropriate weight. To achieve a global model with high accuracy, the committee leader tests the accuracy of the models based on its local data before aggregation in DBAFL. Assuming \mathcal{A}_L^t and \mathcal{A}_G^{t-1} denote the test accuracy of the local model at time t and that of the global model at time $t-1$, respectively, ϵ^t is defined as

$$\epsilon^t = \frac{\mathcal{A}_L^t}{\mathcal{A}_G^{t-1}}. \quad (1)$$

Considering the dynamic scaling factor ϵ^t , the new global model at time t is calculated by

$$w_G^t = \frac{w_G^{t-1} + \epsilon^t \times w_L^t}{1 + \epsilon^t}. \quad (2)$$

From Eq. 2, it is straightforward that a greater value of ϵ means a higher weight of the local model. If the local model has higher accuracy than the global model, the committee leader increases ϵ to assign the local model with higher weight, and vice versa.

Since the committee leader is re-elected on a regular basis, as explained in Section III-D, assessing the model accuracy using local data by the committee leader is neutral and efficient while preserving data privacy. For example, as shown in Fig. 3, after receiving the global model w_G^0 from RSU 1 and the local

model w_L^1 from RSU 2, the committee leader, RSU 3, tests the accuracy of w_G^0 and w_L^1 based on its local data. Due to the disparity in data samples across nodes, the model accuracy assessing on RSU 3 is fairer than on RSU 1 or RSU 2. Besides, to strengthen the generality of the global model, a higher committee leader election frequency could be used.

Algorithm 1 Dynamic Scaling Factor

```

1: function INITIALIZATION ▷ On the first RSU
2:   initialize  $w_L^0$  as  $w_G^0$ 
3:   upload  $\text{Hash}(w_L^0)$  and  $\text{Hash}(w_G^0)$  to the blockchain
4:   save  $w_L^0$  and  $w_G^0$  to the distributed database
5: end function
6:
7: function CLIENTUPDATE ▷ On local nodes
8:   for each local epoch in  $E$  do
9:     download  $w_G^{t-1}$  from the nearby RSU
10:     $w_L^t \leftarrow \text{LocalTrain}(w_G^{t-1}, \text{localTrainData})$ 
11:    upload  $\text{Hash}(w_L^t)$  to the blockchain
12:    upload  $w_L^t$  to the nearby RSU
13:   end for
14: end function
15:
16: function AGGREGATION ▷ On the committee leader
17:   wait  $w_L^t$  in the distributed database
18:    $\mathcal{A}_L^t \leftarrow \text{LocalTest}(w_L^t, \text{localTestData})$ 
19:    $\mathcal{A}_G^{t-1} \leftarrow \text{LocalTest}(w_G^{t-1}, \text{localTestData})$ 
20:    $\epsilon^t \leftarrow \mathcal{A}_L^t / \mathcal{A}_G^{t-1}$ 
21:    $w_G^t = (w_G^{t-1} + \epsilon^t \times w_L^t) / (1 + \epsilon^t)$ 
22:   upload  $\text{Hash}(w_G^t)$  to the blockchain
23:   save  $w_G^t$  to the distributed database
24: end function

```

Algorithm 1 shows the implementation details of the dynamic scaling factor in DBAFL. There are three functions in DBAFL: initialization (Lines 1 to 5), client update (Lines 7 to 14), and aggregation (Lines 16 to 24). The initialization process runs on the first RSU of the smart public transportation system, which trains a local model w_L^0 as the first global model w_G^0 , as shown in Line 2. After uploading hash values of the models to the blockchain, the original models are stored in the distributed database on RSUs, as shown in Lines 3 and 4.

Before training its new local model w_L^t , each local node downloads the latest global model w_G^{t-1} from the nearby RSU, as shown in Lines 9 and 10. After training, each local node uploads the hash value of the local model $\text{Hash}(w_L^t)$ to the blockchain and uploads the original local model w_L^t to the nearby RSU, as shown in Lines 11 and 12. The loop continues if the local epoch E is not reached, as shown in Lines 8. Note that the time t in the client update function (running on local nodes) does not one-to-one correspond to the one in the aggregation function (running on the committee leader), due to the asynchronous aggregation strategy. w_G^{t-1} refers to the latest global model downloaded from the nearby RSU.

From the view of the committee leader, the aggregation progress starts when a new local model w_L^t is uploaded to the distributed database, as shown in Line 17. After testing based on the local data, the accuracies of w_L^t and w_G^{t-1} are

obtained, as shown in Lines 18 and 19. Then, the dynamic scaling factor ϵ^t is calculated according to Eq. 1, as shown in Line 20. Following that, a new global model w_G^t is calculated according to Eq. 2, as shown in Line 21. Finally, the committee leader uploads the hash value of the global model $\text{Hash}(w_G^t)$ to the blockchain and save the original global model w_G^t to the distributed database, as shown in Lines 22 and 23.

D. Committee-Based Consensus Algorithm

In DBAFL, a new committee leader is elected after several new blocks are generated. Specifically, the frequency of electing new committee leaders increases as the reliability requirements grow. The identity of the new committee leader is calculated by the hash value of the latest block.

As shown in Fig. 3, assuming the genesis block Block_0 is generated on RSU 1, the consensus algorithm in the blockchain ensures the replicated blocks on the other nodes are identical as the original Block_0 on RSU 1. Based on the hash value of Block_0 , i.e. $\text{Hash}(\text{Block}_0)$, all nodes acquire the identity of the new committee leader by

$$\text{ID}_L^1 \equiv \text{Hash}(\text{Block}_0) \pmod{M}, \quad (3)$$

where M is the total number of RSUs in DBAFL. Assuming $\text{ID}_L^1 = 3$, RSU 3 is elected as the new committee leader at Block_1 and is placed in charge of aggregating and generating subsequent global models. The election frequency of the committee leader is the reciprocal of the number of blocks to wait before electing a new committee leader. Assume the frequency of the committee leader election is $1/10$, which means that the identity of the new committee leader is calculated in the same way as soon as 10 blocks are appended to the blockchain. Take $\text{ID}_L^{11} = 2$ as an example, RSU 2 is responsible for generating global models in Block_{11} to Block_{20} .

Let the hash value of the latest block at time t is $\text{Hash}(\text{Block}_{t-1})$ and the identity of RSU m is ID_m^t . The probability that RSU m becomes the leader at t is denoted as $P_L(\text{ID}_m^t)$ and is calculated by

$$P_L(\text{ID}_m^t) = \frac{P[\text{Hash}(\text{Block}_{t-1}) \pmod{M} \equiv \text{ID}_m]}{\sum_{j=1}^M P[\text{Hash}(\text{Block}_{t-1}) \pmod{M} \equiv \text{ID}_j]}. \quad (4)$$

The duration of a specific RSU being a leader is limited to prevent it from creating forks on the blockchain and doing evil. Therefore, allowing all RSUs to have the same chance of becoming the leader is the best way to safeguard the system. Gini coefficient, a statistical measure of wealth inequality, is adopted to evaluate inequality in the probability of RSUs becoming a leader in DBAFL, which is calculated by

$$G(t) = \frac{\sum_{m=1}^M \sum_{j=1}^M |P_L(\text{ID}_m^t) - P_L(\text{ID}_j^t)|}{2 \sum_{m=1}^M \sum_{j=1}^M P_L(\text{ID}_j^t)}. \quad (5)$$

It is empirically proved that when adopting SHA-256, a widely used hash function, the non-randomness percentage of the hash output is 31.25% [36]. Accordingly, it is trivial to know that $G(t)$ is less than 0.3125, which is close to 0 and demonstrates that the probability of any RSUs becoming a leader in DBAFL is sufficiently even. With more hash functions are developed,

adopting a more random hash function increases the equality level in the probability of RSUs becoming a leader and subsequently improves the security level of DBAFL.

The original models are stored in the distributed database on RSUs for buses to download. The hash values of the models are stored in the blocks and synchronized to all nodes for the purpose of validating the original model. If the downloaded local model is modified and inconsistent with the hash value stored on the blockchain, the committee leader would ignore it and subsequent local models from that node until a new committee leader is elected. Besides, the procedure of the global model aggregation is also verifiable by all committee members, preventing the committee leader from doing evil.

IV. MODEL ANALYSIS

In this section, DBAFL is theoretically analyzed from several aspects, including convergence, reliability, latency, mobility, and complexity.

A. Convergence Analysis

Assume there are K nodes in DBAFL and \mathcal{D}_k is the local data on node k . The number of samples on node k is $n_k = |\mathcal{D}_k|$. N is the total number of samples across K nodes, which is calculated by $N = \sum_{k=1}^K |\mathcal{D}_k|$. Assume that $\forall k \neq k', \mathcal{D}_k \cap \mathcal{D}_{k'} = \emptyset$. The local empirical loss of node k is:

$$h_k(w_k) = \frac{1}{n_k} \sum_{i \in \mathcal{D}_k} \ell_i(w_k), \quad (6)$$

where $\ell_i(w_k)$ is the corresponding loss function for data i and w_k is the local model parameter. Considering the existence of ϵ , the central objective function is calculated as:

$$F(w) = \sum_{k=1}^K \frac{\epsilon_k}{K} h_k(w_k). \quad (7)$$

where w is the aggregated global model. The goal of Eq. 7 is to find a model that satisfies $w_* = \arg \min_{w \in \mathbb{R}^d} F(w)$.

Following to [6], suppose that $F(w)$ is L -smooth and μ -strongly convex. The local functions $h_k(w)$ are B -locally dissimilar at w , then:

$$F(w^{t+1}) - F(w^t) \leq -\nabla F(w^t)^\top \eta_k^t \frac{\epsilon'_k}{K} \nabla h_k(w^t) + \frac{L}{2} \|\eta_k^t \frac{\epsilon'_k}{K} \nabla h_k(w^t)\|^2, \quad (8)$$

where $\eta_k = \frac{2\mu N'}{LB^2 n'_k}$. μ is a non-negative value that satisfies $\mathbb{E}(\nabla h_k(w)) \leq \|\nabla F(w)\|$. Since $\forall \epsilon_k > 0$, $m_k = \eta_k^t \frac{\epsilon'_k}{K} > 0$. Assuming that $F(w)$ is bounded below, with the local bounded gradient dissimilarity defined in Chen *et al.* [6], it is trivial to know that,

$$\mathbb{E}(F(w^{t+1})) - F(w^t) \leq -m_k \left(\mu - \frac{m_k LB^2}{2} \right) \|\nabla F(w^t)\|^2 \quad (9)$$

is still monotonically increasing. In DBAFL, the accuracy of the initial global model must be greater than 1%. Therefore,

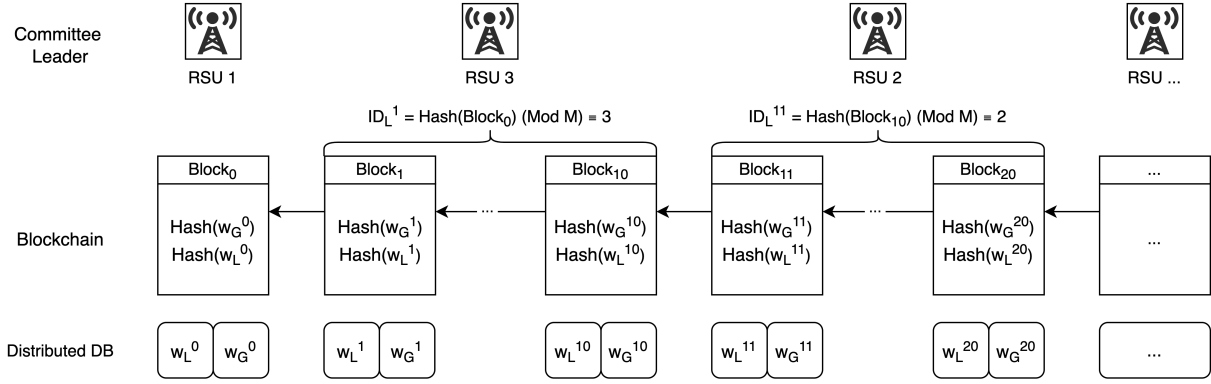


Fig. 3. The committee leader is decided by the hash value of the latest block. The hash values of the models are stored in the blockchain while the original models are stored in distributed databases on RSUs. The relationship between the models in distributed databases and hash values on the blockchain is demonstrated.

$\epsilon_k < 100$. Assume there are at least 100 total training samples among all nodes, $\epsilon'_k < K$. Therefore, $m_k = \eta_k^t \frac{\epsilon'_k}{K} < \eta_k^t$ and

$$-m_k \left(\mu - \frac{m_k LB^2}{2} \right) < -\eta_k^t \left(\mu - \frac{\eta_k^t LB^2}{2} \right). \quad (10)$$

So far, ϵ is already canceled out. As a result, the subsequent proofs are the same as the proofs of Theorem 1 and Theorem 2 in Chen *et al.* [6]. Finally, it is proven that after E epochs, DBAFL converges.

B. Reliability Analysis

1) *Hash Values on Blockchain*: The benefits of uploading models to the blockchain instead of a centralized aggregation server are as follows: i) The consistency and reliability of global models are guaranteed since the data in the blockchain is immutable; ii) The training process becomes transparent and auditable, preventing nodes from doing evil; iii) Buses become trustable due to the existence of the consensus algorithm and the smart contract. Time efficiency is critical for smart public transportation systems, especially when training updated ML models for traffic condition prediction or driver assistance. Since the blockchain is resource-intensive, local nodes in DBAFL only upload the hash values of the models to the blockchain. The aforementioned benefits are preserved, as the model history is still traceable by the hash values in the blockchain and the original models are downloadable and verifiable by all local nodes. Furthermore, this mechanism greatly reduces the storage redundancy in the blockchain as well as the storage requirements for buses.

2) *Attack Resistance*: The design of DBAFL is primarily resistant to poisoning and DDoS attacks. When launching poisoning attacks, the attackers manipulate the parameters of local models and upload them to the global model, causing the accuracy of the global model to decrease [4]. However, the committee leader is able to identify the malicious local models by testing their accuracy locally. As a result, the committee leader will assign them relative low weight, which defends poisoning attacks to a certain extent. Since the committee-based consensus algorithm periodically elects a new leader based on the hash value of the latest block, the accuracy

test result is ensured to be reliable and unbiased. In addition, DBAFL introduces a stricter defense strategy that discards local models with an accuracy below a specific threshold to further reduce the influence of malicious local models. DDoS attacks primarily aim to disrupt the centralized aggregation server in traditional FL schemes by flooding [37]. In DBAFL, the periodically changed committee leader replaces the centralized aggregation server in classic FL, reducing the probability of being targeted by traffic flooding in DDoS attacks.

3) *Leader Election*: A more frequent committee leader election leads to the increased reliability of DBAFL and the higher generality of the global model. However, it is almost impossible to guarantee efficiency if the committee leader is elected too frequently. Considering the mobile network is unstable, the network latency is likely to result in committee leader identities inconsistent and forks in the blockchain during block propagation. Aside from that, block size has an impact on efficiency as well. The decreased block size enables more frequent committee leader elections, which results in more blocks propagated in the blockchain and additional network overhead.

4) *Unstable Mobile Network*: Buses may fall offline unexpectedly in an unstable mobile network. As a comparison, RSUs equipping with backup for disaster recovery are more stable. Therefore, only RSUs are committee members and eligible to be the committee leader, ensuring a stable global model aggregation process. A bus that falls offline unexpectedly will not affect the training process on other nodes in DBAFL due to its asynchronous aggregation strategy. Storing models in InterPlanetary File System (IPFS) is a promising solution to further improve data reliability [38] and is left for future work.

C. Latency Analysis

According to [39], in a classic blockchain-based FL scheme, the latency of a training round is the sum of local training T_{local}^e , model uploading T_{up}^e , model aggregation T_{ag}^e , block generation T_{bg}^e , block propagation T_{bp}^e , and model downloading T_{dn}^e . Therefore, the latency of e -th epoch T^e is given as

$$T^e = T_{\text{local}}^e + T_{\text{up}}^e + T_{\text{ag}}^e + T_{\text{bg}}^e + T_{\text{bp}}^e + T_{\text{dn}}^e. \quad (11)$$

Specifically, in the local training phase, nodes do not need communication with others. Since the asynchronous aggregation strategy does not wait for the local training on nodes before aggregation, the local training latency T_{local}^e is ignored in DBAFL. As illustrated in Line 11, 12, and 17 of Algorithm 1, the latency of model uploading phase is composed of three parts: local model uploading $T_{\text{up_model}}^e$ from buses to RSUs, model hash uploading $T_{\text{up_hash}}^e$ from buses to RSUs, and model synchronization $T_{\text{sync_model}}^e$ among RSUs. Therefore, the latency of model uploading phase T_{up}^e is expressed as

$$T_{\text{up}}^e = T_{\text{up_model}}^e + T_{\text{up_hash}}^e + T_{\text{sync_model}}^e \\ = \frac{S_w}{\mathbb{B}_M \log_2(1 + \gamma_M)} + \frac{S_{\text{hash}}}{\mathbb{B}_M \log_2(1 + \gamma_M)} + \frac{S_w}{\mathbb{B}_E}, \quad (12)$$

where S_w is the size of the model, S_{hash} is the size of the model hash, \mathbb{B}_E and \mathbb{B}_M are the bandwidth allocations of the Ethernet network and the mobile network, respectively, and γ_M is the received signal-to-noise ratio (SNR) of the devices in the mobile network. As RSUs are connected with each other through a high-speed Ethernet, there is no SNR considered in $T_{\text{sync_model}}^e$.

After aggregation, the hash value of the global model is uploaded to the blockchain while the original global model is synchronized among RSUs, as shown in Line 22 and 23 of Algorithm 1. Assuming the time of processing aggregation is negligible compared with the communication delays, the latency of model aggregation phase T_{ag}^e is calculated as

$$T_{\text{ag}}^e = T_{\text{up_hash}}^e + T_{\text{sync_model}}^e = \frac{S_{\text{hash}}}{\mathbb{B}_M \log_2(1 + \gamma_M)} + \frac{S_w}{\mathbb{B}_E}. \quad (13)$$

In order to improve efficiency, the committee-based consensus algorithm in DBAFL does not involve mining or communicating during the block generation process, as demonstrated in Section III-D. Therefore, the latency of generating blocks T_{bg}^e only involves a small amount of time spent computing hash values and is considered negligible in comparison to the communication delays. Thereafter, the newly generated block is propagated throughout the network with latency

$$T_{\text{bp}}^e = \frac{S_{\text{block}}}{\mathbb{B}_M \log_2(1 + \gamma_M)}, \quad (14)$$

where S_{block} is the size of the block. Finally, as shown in Line 9 of Algorithm 1, buses download the new global model from the nearby RSU with latency

$$T_{\text{dn}}^e = \frac{S_w}{\mathbb{B}_M \log_2(1 + \gamma_M)}. \quad (15)$$

Moreover, compared with an asynchronous federated learning scheme, the additional communication latency brought by the blockchain T_{bc}^e is

$$T_{\text{bc}}^e = 2T_{\text{up_hash}}^e + 2T_{\text{sync_model}}^e + T_{\text{bp}}^e, \quad (16)$$

due to the requirements of uploading hash values of global and local models, synchronizing local and global models among RSUs, and releasing the new block. Since the hash size is much smaller than the model size, S_{hash} and S_{block} are much smaller than S_w . Thus, $T_{\text{up_hash}}^e + T_{\text{bp}}^e \ll T_{\text{up}}^e + T_{\text{dn}}^e$. Moreover, by increasing the bandwidth among RSUs \mathbb{B}_E , $T_{\text{sync_model}}^e$ is

easy to be reduced to very small. As a result, T_{bc}^e is smaller than T^e and acceptable in public transportation scenarios.

D. Mobility Analysis

Assume buses are traveling on a road in a built-up area, where the 5G network coverage of an RSU is 300 meters and the vehicle speed limit is 60 km/h [40]. By calculating, the connection of a running bus to an RSU lasts 18 seconds at most. Due to the device heterogeneity, it is hard to determine how long it will take a bus to finish training a local model. In DBAFL, the training of local models is independent for each bus due to the asynchronous aggregation strategy, which means that no network connection or waiting for others is required during the training process. After training, buses need to upload the local model to the nearby RSU and the hash value to the blockchain before downloading a new global model from the nearby RSU. As evaluated in Section V-B2, the communication time cost in each training round of DBAFL is always less than 5 seconds, which is much less than the limitation of 18 seconds. After receiving the local model, the committee leader performs aggregation locally and generates a new global model, which is shared with other RSUs without effects from the mobility of buses. Besides, the leader election among committee members (RSUs) is also not affected by the mobility of buses. Therefore, considering the mobility of buses, DBAFL is still feasible in smart public transportation systems.

E. Complexity Analysis

As the collected data changes over time, models are trained on a regular basis. Assuming the newly arrived data size on a bus is n , the computational complexity of training on the bus is $\mathcal{O}(n)$. Since each bus has to perform training for E epochs, the computational complexity of DBAFL on each bus is $\mathcal{O}(nE)$. Considering DBAFL enables buses to train parallelly without waiting for models from others, the overall computational complexity of DBAFL is $\mathcal{O}(nE)$, which is acceptable.

Compared with classic FL, DBAFL has an additional communication complexity of uploading hash of models to the blockchain and electing new committee leaders. As the hash values are small enough without effects of the model size, it is easy to be packed into blocks and broadcast to nodes through the P2P protocol. Since the identity of the new committee leader is determined by the hash value of the specific block, no more network communication is required after the block is broadcasted to local nodes in IoV networks. Therefore, the communication complexity for each training round is $\mathcal{O}(\log K)$, where K is the number of nodes in DBAFL. Besides, the blockchain could be deployed purely on RSUs to reduce the communication complexity of buses at the cost of certain security and credibility. In that situation, the communication complexity for each training round is $\mathcal{O}(\log M)$, where M ($M \ll K$) is the number of RSUs.

V. SYSTEM EVALUATION

In this section, experiments are conducted from three aspects, including learning performance, efficiency, and reliability.

TABLE I
THE EXPERIMENT PARAMETER SETTINGS

Parameter	Value
The number of nodes K	5
The local data size B	1500
The number of epochs E	50
The learning rate η	0.01
The static scaling factor ϵ	{0.5, 1.0, 1.5}
The time to wait before creating a block	2s
The maximum number of messages in a block	10
The maximum bytes of messages in a block	10MB

bility, to evaluate DBAFL on IoV networks and answer the following research questions:

- **RQ1:** How well does DBAFL improve learning performance compared with state-of-the-art schemes?
- **RQ2:** Is there any advantage of DBAFL in efficiency compared with state-of-the-art schemes?
- **RQ3:** Is DBAFL reliable enough to resist poisoning and DDoS attacks?

A. Experiment Setup

Five virtual machines (VM) and four Raspberry PI B4 devices are set up as the experiment environment. Each VM has 8 CPU cores and 8GB RAM to simulate an RSU. Each Raspberry PI B4 has 4 CPU cores and 8GB RAM to simulate a vehicle with limited computing resources. In terms of software configuration, the Ubuntu 20.10 operating system is deployed on all nodes. ML models are trained with PyTorch v1.8.1 based on Python 3.8. The smart contract is developed on Hyperledger Fabric v2.3.0, an open-source blockchain framework, to orchestrate model training and aggregation on nodes and accept model hash values. Besides, a RESTful service is developed on Express.js v4.17.1, allowing local nodes to upload or download the hash values of models from the blockchain. The implementation details are available at <https://github.com/xuchenhao001/AFL>.

The default parameter settings for experiments are shown in Table I. The number of nodes on a road is assumed to be five by default, including an RSU and four buses traveling under the network coverage of the RSU. In experiments, the number of buses and RSUs ranges from one to four. Similar to [3], [11], [35], the local data size B is 1500, the number of local epochs E is 50, and the learning rate η is 0.01. To examine the effectiveness of the dynamic setting strategy, the value of ϵ is set to static, including 0.5, 1.0, and 1.5, to reveal the impact of under-, equal-, and over-weighted stale local models. According to the default parameter settings in Hyperledger Fabric [41], a new block is generated when any of the following conditions is reached: the waiting time for the next invoke reaches 2 seconds, the number of invokes reaches 10, or the block size reaches 10 MB.

The ML models are trained on two benchmark datasets (i.e. CIFAR-10 [11] and FMNIST [42]) and one real-world dataset (i.e. LOOP [43]). Specifically, the LOOP dataset contains the speed information collected by the inductive loop detectors

deployed on freeways in the Seattle area at intervals of 5 minutes. The ML models include MLP, CNN, and LSTM.

To evaluate DBAFL, several state-of-the-art schemes are included in the scope for comparison.

- 1) **BSFL:** The synchronized version of DBAFL without the dynamic scaling factor. Blockchain is included.
- 2) **ASOFED:** An AFL scheme with static decay coefficient balancing the previous and current gradients [6]. Blockchain is not included.
- 3) **BDFL:** An AFL scheme with all models saved in the blockchain [30].
- 4) **APFL:** A semi-AFL scheme with reduced the communication frequency [10]. Blockchain is not included.
- 5) **FedAVG:** The traditional synchronous FL scheme [3]. Blockchain is not included.
- 6) **Local:** The traditional local training scheme that each node trains the ML model on local data without communication. Blockchain is not included.

Average test accuracy is calculated by averaging the accuracy of the local models on all nodes in a fixed-time interval. The average loss is calculated in the same way based on the mean square error (MSE). The average time is calculated by averaging the time cost of all nodes in each training round. The average time per iteration is calculated by averaging the time cost of all nodes across all training rounds.

To answer *RQ1*, the average test accuracy is compared with state-of-the-art schemes when different models, datasets, and IoV network settings are applied. Specifically, there are two aspects of IoV network settings: (1) using different numbers of IoT devices and VMs to mimic the differences in computing resources among vehicles and RSUs; (2) distributing different sizes of local data on VMs to mimic the disparity of data collected among nodes. The node with a large volume of data is the big node, whose local data size is set to 5000. For clear comparison, the local data size for a small node is set to 500. In addition, to validate the effectiveness of the dynamic setting, the average test accuracy with the scaling factor adopted under three static settings, including 0.5, 1.0, and 1.5, is compared with that under the dynamic setting.

To answer *RQ2*, the average overall time cost in each training round is compared when adopting different models and datasets in experiments. To further investigate the communication overhead brought by the blockchain, the average communication time cost in each training round is also compared. When training the CNN model on the CIFAR-10 dataset, the average time costs on different stages and in different scales of networks are compared.

To answer *RQ3*, Node 5 randomly adjusts the parameters in local models before sending them to the committee leader to simulate poisoning attacks. The test accuracy of DBAFL with different levels of defense strategies is compared with that of the classic AFL scheme without any defense strategy. Moreover, the average test accuracy of DBAFL and that of the classic AFL scheme are compared at different levels of DDoS attacks, especially when 80% or 90% of the total traffic is the DDoS attack traffic.

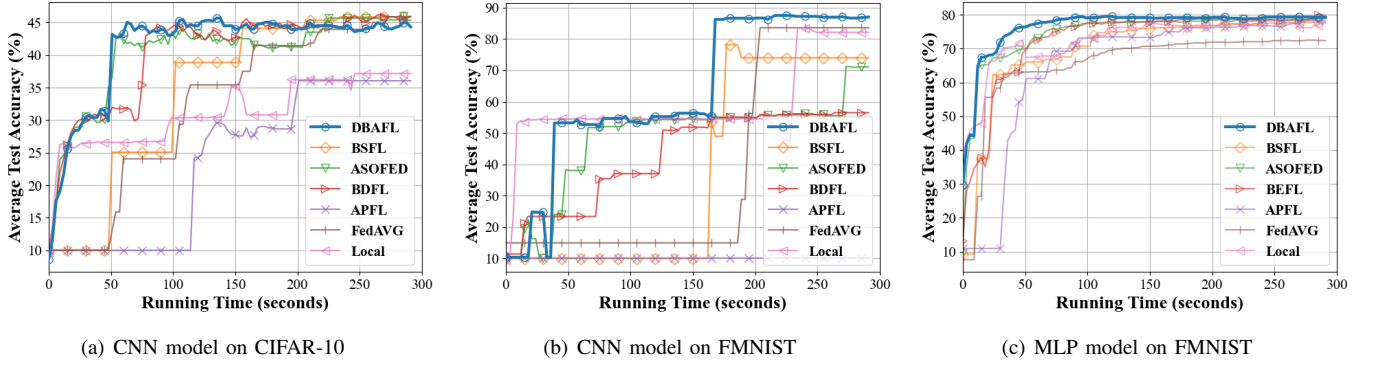


Fig. 4. Compare the average test accuracy of models in DBAFL with that of models in other schemes. There are five nodes in the network, two of which are vehicles while others are RSUs.

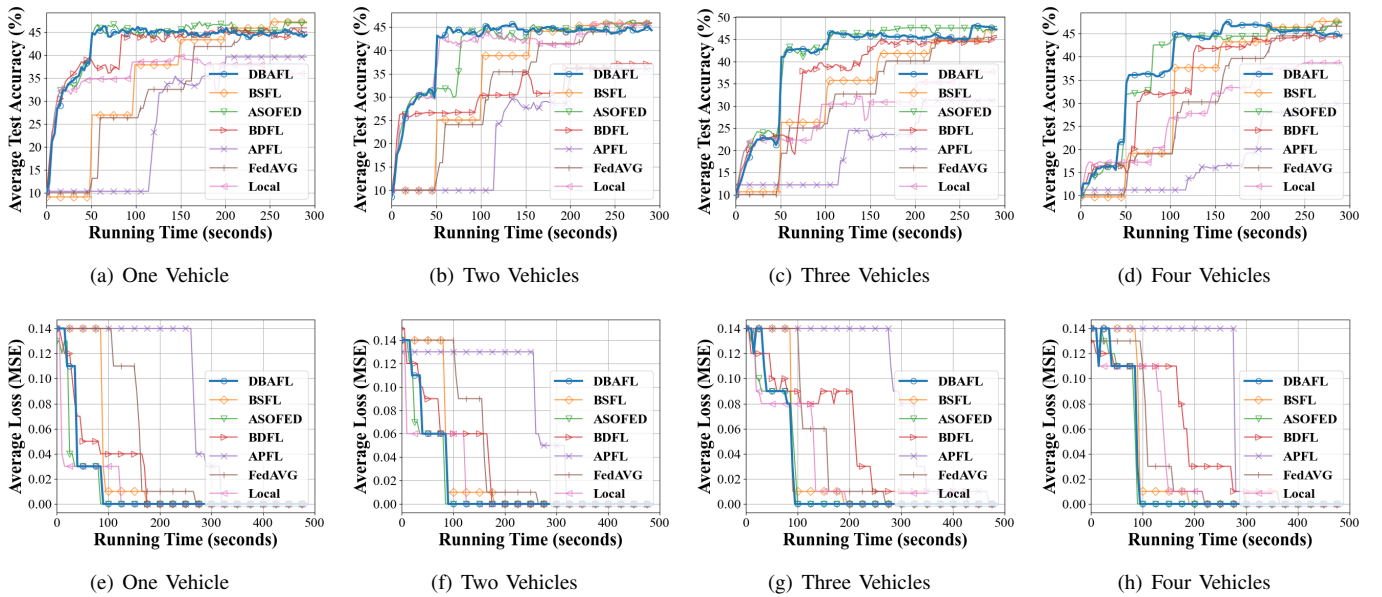


Fig. 5. Compare the average test accuracy when different numbers of vehicles participate in training. There are five nodes in the network. Top row: The average test accuracy when train CNN on CIFAR-10. Bottom row: The average loss evaluated by mean squared error when train LSTM on LOOP.

B. Results Analysis

1) *RQ1. Convergence Speed and Model Accuracy:* As shown in Fig. 4, initially, the convergence speed of DBAFL is a little lower than that of the local training scheme but higher than the other ones. Subsequently, relatively early in the cycle of the tests, the average test accuracy of DBAFL steps up to an optimal level and converges faster than all other schemes. The step-up is due to the contribution of stale local models from vehicles. When training the CNN model, the step-up happens earlier on CIFAR-10 (at around the 50th second) than that on FMNIST (at around the 160th second), revealing that FMNIST is more complex and harder for vehicles to train. In addition, on the FMNIST dataset, DBAFL converges faster when the trained model is MLP, rather than CNN, because the MLP model is much simpler than the CNN model. Finally, the average test accuracy of DBAFL when training CNN and MLP models on two different datasets is always optimal compared with that of other schemes, which reveals the stable learning

performance of DBAFL.

When training the CNN model on the CIFAR-10 dataset, as shown in Fig. 5 (a) to (d), the advantage of DBAFL in terms of convergence speed is more obvious compared with BSFL, BDFL, APFL, and FedAVG, under the circumstance of fewer vehicles. For example, the convergence time of DBAFL is around 150 seconds earlier (note the 50th second and the 200th second marks) than that of BSFL and FedAVG when only one vehicle is in the network, while the convergence time of DBAFL is around 50 seconds earlier (note the 150th second and the 200th second marks) than that of BSFL and FedAVG when four vehicles are in the network. The reason is that more nodes with rich computing resources involved in the network contribute more local models at the early stage, resulting in higher convergence speeds. When comparing the average test accuracy of models, DBAFL performs more stable (at around 45%) than the local training scheme (from around 40% down to around 20%) as the number of vehicles increases. This is

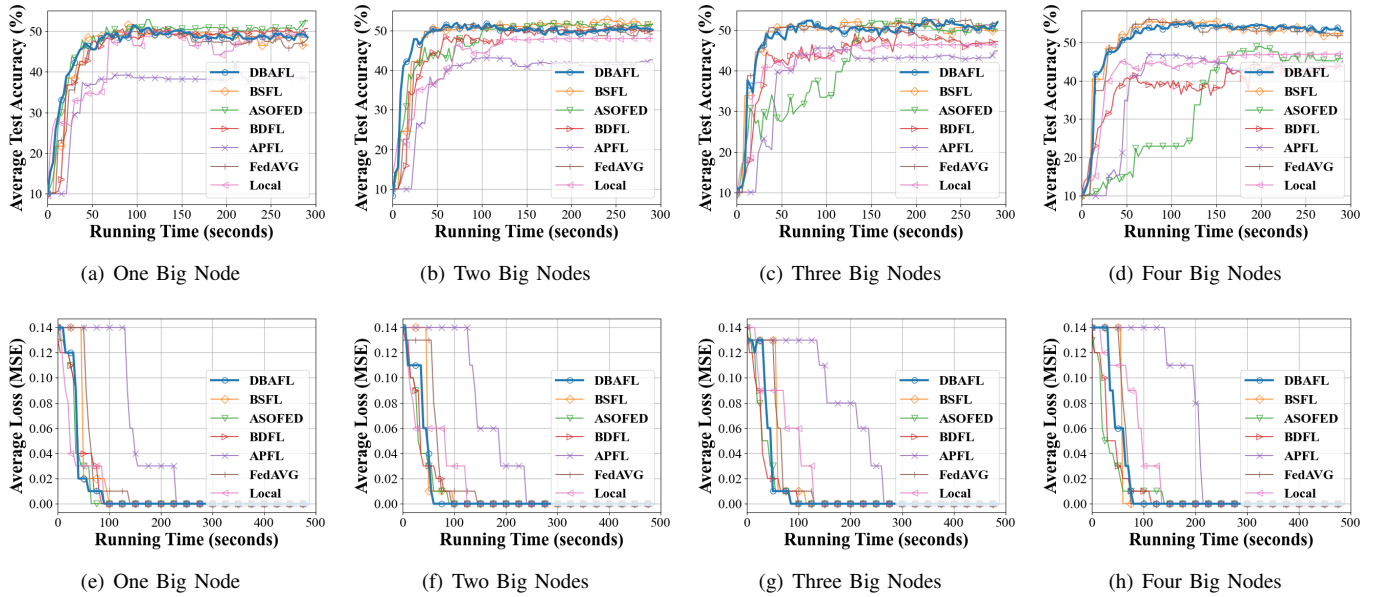


Fig. 6. Compare the average test accuracy when different numbers of big nodes participate in training. There are five nodes in the network. Top row: The average test accuracy when train CNN on CIFAR-10. Bottom row: The average loss evaluated by mean squared error when train LSTM on LOOP.

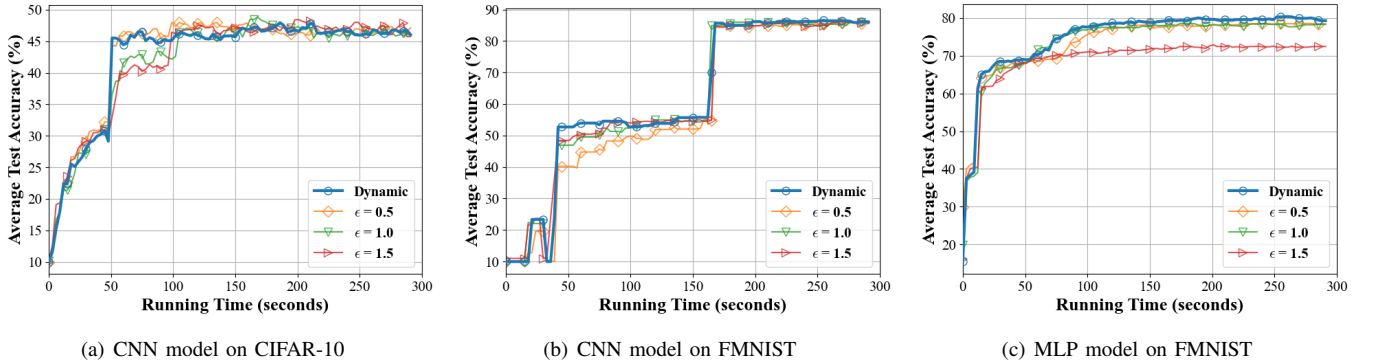


Fig. 7. Compare the average test accuracy under dynamic scaling factor setting with that under static scaling factor settings. There are five nodes in the network, two of which are vehicles while others are RSUs.

because a lagging node with limited computing resources is unable to learn information from the high-performance nodes in the network, ASOFED and BDFL have decreased model accuracy and slowed convergence speed. This is because too much training data on big nodes slows down their training process, while the local models from small nodes are not weighted appropriately during the aggregation. When training the LSTM model on the LOOP dataset, as shown in Fig. 5 (e) to (h), the convergence speed of DBAFL also decreases (as expected) with the increase of vehicles in the network, although the final convergence time is almost identical. The reason is that the LSTM model fits the LOOP dataset easily and converges after the first round of aggregation, while the finish time of the first round of training on vehicles is almost the same (at around the 100th second mark).

To assess the impact of local data size on average test accuracy, big nodes (nodes with a lot of data) and small nodes (nodes with a small amount of data) have 5000 and 500 training samples, respectively. As shown in Fig. 6 (a) to (d), DBAFL is able to achieve the optimal model accuracy com-

pared with the state-of-the-art schemes. With more big nodes in the network, ASOFED and BDFL have decreased model accuracy and slowed convergence speed. This is because too much training data on big nodes slows down their training process, while the local models from small nodes are not weighted appropriately during the aggregation. When training the LSTM model on the LOOP dataset, as shown in Fig. 6 (e) to (h), the convergence speed of DBAFL is barely affected by any increase in the number of big nodes in the network, which is determined by the fastest node in the network. Nevertheless, compared with other schemes, DBAFL is always the fastest to converge.

Compared with static settings, the dynamic setting strategy allows DBAFL to assign an optimal scaling factor during the training process, resulting in the best convergence speed and model accuracy in all situations, as shown in Fig. 7. In addition, the ideal static scaling factor setting, which varies when training various models on different datasets, follows no

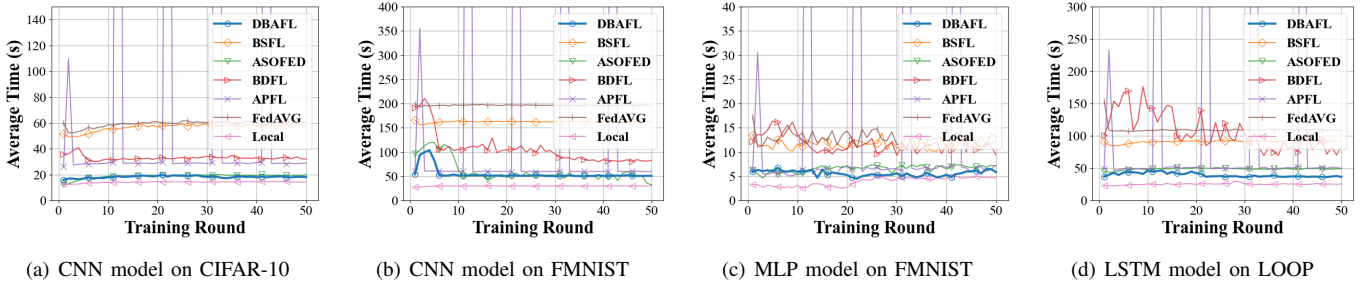


Fig. 8. Compare the average overall time cost in each training round of DBAFL with other schemes. There are five nodes in the network, two of which are vehicles while others are RSUs.

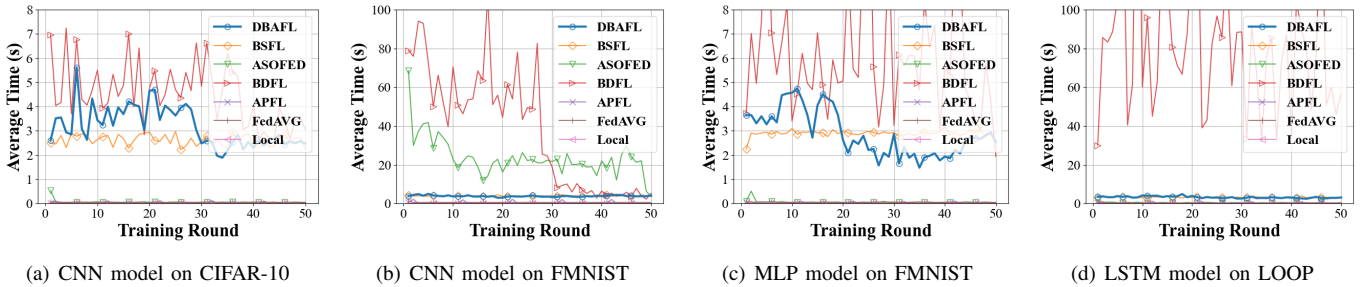


Fig. 9. Compare the average communication time cost in each training round of DBAFL with other schemes. There are five nodes in the network, two of which are vehicles while others are RSUs.

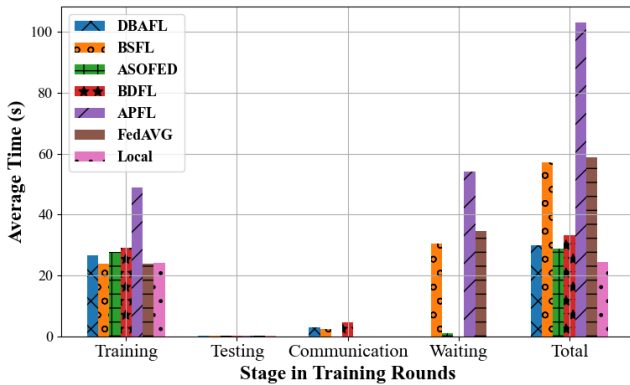


Fig. 10. Compare the average time cost of four different stages, including training, test, communication, and waiting, in the training round when training the CNN model on the CIFAR-10 dataset. Training: Nodes train their local models; Testing: Nodes test the accuracy of the local and global models; Communication: Nodes upload and download local and global models; Waiting: Nodes wait for the global model to be aggregated. Total: The sum of the average time cost of four stages. There are five nodes in the network, two of which are vehicles while others are RSUs.

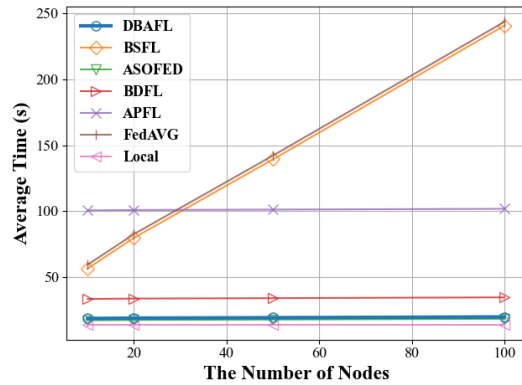


Fig. 11. Compare the average time cost when training the CNN model on the CIFAR-10 dataset with different numbers of nodes in the network. All nodes are with the same computing resources as RSUs.

obvious pattern. Take the CNN model as an example: the ideal static setting for the scaling factor when training on CIFAR-10 is 0.5, whereas it is 1.5 when training on FMNIST. Because the learning process is random, all nodes have the same probability of discovering an appropriate learning direction, regardless of computing resources or local data size. When the fast nodes discover the best learning direction first, it is desirable to set the scaling factor to a value less than 1.0 in order to reduce the impact of stale local models. On the contrary, it is preferential to set the scaling factor to a value

greater than 1.0 to amplify the impact of remarkable local models when the fast nodes initially identify the worst learning direction.

Result 1: DBAFL has a superior convergence speed and optimal model accuracy compared with state-of-the-art schemes.

2) *RQ2. Time Costs:* As shown in Fig. 8, DBAFL has the lowest overall time cost in each training round compared with state-of-the-art schemes in all situations. Especially, when training the CNN model on the FMNIST dataset, the average overall time cost of DBAFL in each training round (around

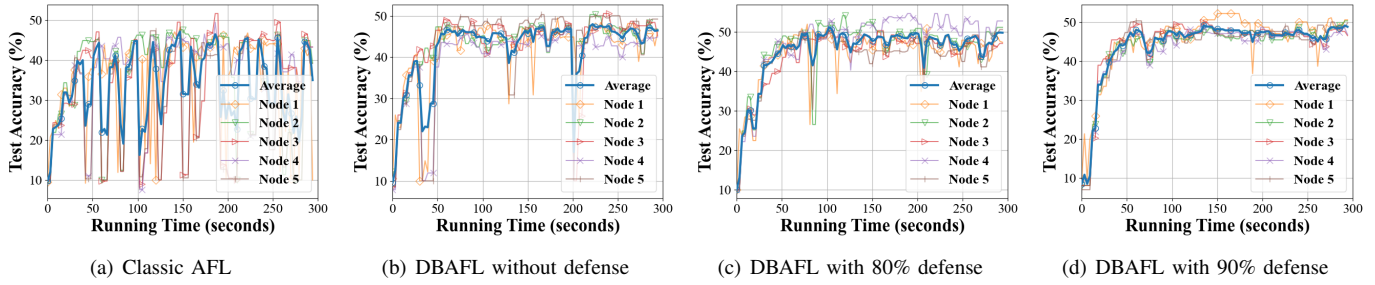


Fig. 12. When Node 5 launches poisoning attacks, compare the average test accuracy of models in DBAFL at various degrees of defense thresholds with that of models in the classic AFL scheme without any defense.

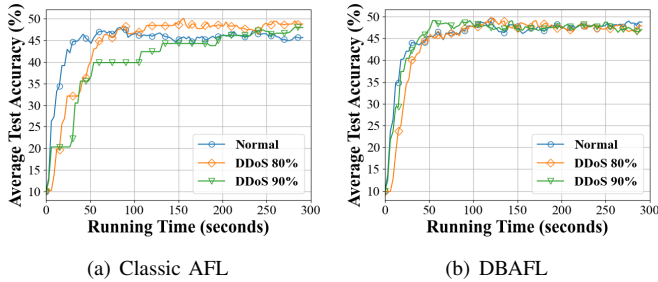


Fig. 13. When suffering different degrees of DDoS attacks, compare the average test accuracy of models in DBAFL with that of models in the classic AFL scheme.

50 seconds) is 150 seconds less than that of FedAVG (around 200 seconds). This is because the asynchronous aggregation strategy shortens the waiting time before aggregation. As a result, the advantage of DBAFL in terms of time cost in each training round becomes ever more apparent if the training process is more time-consuming. In addition, the periodic spike in average overall time cost in APFL is mainly caused by the waiting for the lagging nodes in every 10 rounds of training.

The average communication time cost in each training round is in line with the previous analysis, as shown in Fig. 9. The average communication cost in each training round of DBAFL is higher than that of FedAVG and APFL, and comparable to that of BSFL. This is caused by the additional time cost in the underlying blockchain architecture, including consensus and block propagation. However, it is obvious that DBAFL has a lower average communication time cost than BDFL, since hash values instead of the original models are uploaded to the blockchain. Moreover, compared with the average overall time cost in each training round of classic FL (FedAVG), the additional communication time cost incurred due to blockchain is mostly negligible, especially when training the CNN model on the FMNIST dataset (at 200 seconds compared with 4 seconds). Since the additional communication time cost brought by blockchain is 3 seconds with little variation, the impact of blockchain becomes less as the model training task becomes more complex.

When training the CNN model on the CIFAR-10 dataset, the average time cost at different stages among all training rounds and all nodes is summarized in Fig. 10. In terms of

the training stage, DBAFL has a little higher average time cost than BSFL, FedAVG, and Local Training (around 2.5 seconds higher), which is due to the more frequent aggregation requests sent to the committee leader under the asynchronous aggregation strategy. APFL has the highest average time cost on training (almost twice the time than for the other schemes) due to two training procedures in each training round. In terms of the test stage, it is obvious that all schemes spend very little time (less than 0.3 seconds), implying that the additional accuracy-test stage in DBAFL has a negligible impact on the efficiency of AFL. In terms of the communication stage, the average time cost of DBAFL, BSFL, and BDFL is slightly higher than that of FedAVG, APFL, and Local Training due to the consensus process of the blockchain. However, DBAFL has a minimal time cost in waiting for other nodes, which is similar to ASOFED, BDFL, and Local Training, due to its asynchronous aggregation strategy. On the other hand, BSFL, APFL, and FedAVG waste nearly half of the time in a round waiting instead of training or communicating, resulting in lower training efficiency when compared with DBAFL. After summing the average time cost of training, test, communication, and waiting stages, the total round time of DBAFL is only 0.97 seconds longer than that of ASOFED. This shows that the proposed scheme effectively mitigates the effects of the blockchain.

When increasing the network scale from 10 to 100, the average time cost of a training round is demonstrated in Fig. 11. As the number of nodes in the network increases, high-performance nodes have to wait for more lagging nodes in each training round when adopting synchronous aggregation strategies, implying a longer waiting time. As a result, the schemes utilizing asynchronous aggregation strategies (DBAFL, ASOFED, BDFL, and APFL) have better scalability than those adopting synchronous aggregation strategies (BSFL and FedAVG). Besides, even with the blockchain incorporated, DBAFL achieves the same scalability as the pure AFL scheme ASOFED and has higher scalability than other blockchain-based schemes, due to the adoption of the proposed efficient consensus algorithm.

Result 2: DBAFL spends the shortest time in each training round while making full use of the computing resources

on each node without time wasted waiting for other nodes.

3) *RQ3. Attack Resistance*: As shown in Fig. 12 (a) and (b), the classic AFL scheme has difficulty converging under poisoning attacks, while DBAFL is resistant to poisoning attacks initially to a certain extent. Despite multiple dips during the training process, DBAFL eventually converges at an appropriate accuracy level (at around the 50th second mark). The outcome is consistent with the analysis in Section IV-B, as the committee leader identifies local models with low accuracy and assigns a relatively small scaling factor to them. Moreover, when adopting a stricter defense strategy, for example, discarding local models with accuracy lower than the threshold, the resistance of DBAFL towards poisoning attacks is further improved. As shown in Fig. 12 (c) and (d), when the defense threshold reaches 80% and 90%, both the degree and the number of dips are reduced, as the impacts of poisoned local models are mitigated more thoroughly. In addition, with an increased degree of defense, the average test accuracy of the model is also increased slightly (from 46% to 49%). This reveals that discarding poisoned local models has no side effects for DBAFL, as the global model learns nothing from the poisoned local models.

When suffering DDoS attacks, the aggregation server in the classic AFL scheme becomes unresponsive to aggregation requests, leading to a lower convergence speed of the global model. As shown in Fig. 13 (a), the convergence time increases from 40 seconds to 200 seconds as the DDoS attack traffic increases from 0% to 90%. However, the convergence speed of DBAFL is barely affected even when the DDoS attacks traffic is increased to 90%. This is due to the periodic election of a random committee leader, which reduces the likelihood of the committee leader being the subject of DDoS attacks.

Result 3: DBAFL is natively resistant to both poisoning and DDoS attacks with the potential to improve reliability further.

VI. SUMMARY AND FUTURE WORK

This paper offers a blockchain-based asynchronous federated learning scheme with a dynamic scaling factor, aiming to address the challenges faced by FL on IoV networks in terms of learning performance, efficiency, and reliability. The novel committee-based consensus algorithm in blockchain ensures the reliability of DBAFL with the least cost in communication latency. In conjunction with the efficient asynchronous aggregation strategy, the dynamic scaling factor assigns reasonable weights to stale local models and improves learning performance for DBAFL. Extensive experiments conducted on heterogeneous devices validate the advantages of DBAFL in learning performance, efficiency, and reliability.

Future work includes recovering models when nodes go offline unexpectedly, applying DBAFL on non-independent and -identically distributed (Non-IID) datasets, and designing effective strategies to resist other attacks.

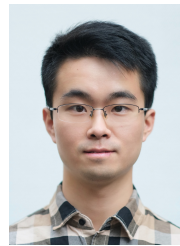
ACKNOWLEDGMENT

Many thanks to Wanping Bai for her time and efforts in helping proofread this paper.

REFERENCES

- [1] Yunlong Lu, Xiaohong Huang, Ke Zhang, Sabita Maharjan, and Yan Zhang. Blockchain empowered asynchronous federated learning for secure data sharing in internet of vehicles. *IEEE Transactions on Vehicular Technology*, 69(4):4298–4311, 2020.
- [2] Xiangjie Kong, Haoran Gao, Guojiang Shen, Gaohui Duan, and Sajal K Das. Fedvcp: A federated-learning-based cooperative positioning scheme for social internet of vehicles. *IEEE Transactions on Computational Social Systems*, 2021.
- [3] Brendan McMahan, Eider Moore, Daniel Ramage, Seth Hampson, and Blaise Aguera y Arcas. Communication-efficient learning of deep networks from decentralized data. In *Artificial Intelligence and Statistics*, pages 1273–1282. PMLR, 2017.
- [4] Chenhao Xu, Youyang Qu, Yong Xiang, and Longxiang Gao. Asynchronous federated learning on heterogeneous devices: A survey. *arXiv preprint arXiv:2109.04269*, 2021.
- [5] Lingjuan Lyu, Jiangshan Yu, Karthik Nandakumar, Yitong Li, Xingjun Ma, Jiong Jin, Han Yu, and Kee Siong Ng. Towards fair and privacy-preserving federated deep models. *IEEE Transactions on Parallel and Distributed Systems*, 31(11):2524–2541, 2020.
- [6] Yujing Chen, Yue Ning, Martin Slawski, and Huzefa Rangwala. Asynchronous online federated learning for edge devices with non-iid data. In *2020 IEEE International Conference on Big Data (Big Data)*, pages 15–24. IEEE, 2020.
- [7] Yang Chen, Xiaoyan Sun, and Yaochu Jin. Communication-efficient federated deep learning with layerwise asynchronous model update and temporally weighted aggregation. *IEEE transactions on neural networks and learning systems*, 31(10):4229–4238, 2019.
- [8] Wentai Wu, Ligang He, Weiwei Lin, Rui Mao, Carsten Maple, and Stephen A Jarvis. Safa: a semi-asynchronous protocol for fast federated learning with low overhead. *IEEE Transactions on Computers*, 2020.
- [9] Xiaofeng Lu, Yuying Liao, Pietro Lio, and Pan Hui. Privacy-preserving asynchronous federated learning mechanism for edge network computing. *IEEE Access*, 8:48970–48981, 2020.
- [10] Yuyang Deng, Mohammad Mahdi Kamani, and Mehrdad Mahdavi. Adaptive personalized federated learning. *arXiv preprint arXiv:2003.13461*, 2020.
- [11] Chenhao Xu, Youyang Qu, Peter W Eklund, Yong Xiang, and Longxiang Gao. Baf: An efficient blockchain-based asynchronous federated learning framework. In *2021 IEEE Symposium on Computers and Communications (ISCC)*, pages 1–6. IEEE, 2021.
- [12] Mansoor Ali, Hadis Karimipour, and Muhammad Tariq. Integration of blockchain and federated learning for internet of things: Recent advances and future challenges. *Computers & Security*, page 102355, 2021.
- [13] Youyang Qu, Shiva Raj Pokhrel, Sahil Garg, Longxiang Gao, and Yong Xiang. A blockchain federated learning framework for cognitive computing in industry 4.0 networks. *IEEE Transactions on Industrial Informatics*, 2020.
- [14] Chenhao Xu, Youyang Qu, Tom H Luan, Peter W Eklund, Yong Xiang, and Longxiang Gao. A light-weight and attack-proof bidirectional blockchain paradigm for internet of things. *IEEE Internet of Things Journal*, 2021.
- [15] Seyed Mojtaba Hosseini Bamakan, Amirhossein Motavali, and Alireza Babaei Bondarti. A survey of blockchain consensus algorithms performance evaluation criteria. *Expert Systems with Applications*, 154:113385, 2020.
- [16] Yinghui Liu, Youyang Qu, Chenhao Xu, Zhicheng Hao, and Bruce Gu. Blockchain-enabled asynchronous federated learning in edge computing. *Sensors*, 21(10):3335, 2021.
- [17] Lei Feng, Yiqi Zhao, Shaoyong Guo, Xuesong Qiu, Wenjing Li, and Peng Yu. Blockchain-based asynchronous federated learning for internet of things. *IEEE Transactions on Computers*, 2021.
- [18] Shuo Yuan, Bin Cao, Mugen Peng, and Yaohua Sun. Chainsfl: Blockchain-driven federated learning from design to realization. In *2021 IEEE Wireless Communications and Networking Conference (WCNC)*, pages 1–6. IEEE, 2021.
- [19] Muhammad Habib ur Rehman, Khaled Salah, Ernesto Damiani, and Davor Svetinovic. Towards blockchain-based reputation-aware federated learning. In *IEEE INFOCOM 2020-IEEE Conference on Computer Communications Workshops (INFOCOM WKSHPS)*, pages 183–188. IEEE, 2020.

- [20] Jiayi Weng, Jian Weng, Jilian Zhang, Ming Li, Yue Zhang, and Weiqi Luo. Deepchain: Auditable and privacy-preserving deep learning with blockchain-based incentive. *IEEE Transactions on Dependable and Secure Computing*, 2019.
- [21] Zhe Peng, Jianliang Xu, Xiaowen Chu, Shang Gao, Yuan Yao, Rong Gu, and Yuzhe Tang. Vfchain: Enabling verifiable and auditable federated learning via blockchain systems. *IEEE Transactions on Network Science and Engineering*, 2021.
- [22] Muhammad Shayan, Clement Fung, Chris JM Yoon, and Ivan Beschastnikh. Biscotti: A blockchain system for private and secure federated learning. *IEEE Transactions on Parallel and Distributed Systems*, 2020.
- [23] Yuzheng Li, Chuan Chen, Nan Liu, Huawei Huang, Zibin Zheng, and Qiang Yan. A blockchain-based decentralized federated learning framework with committee consensus. *IEEE Network*, 2020.
- [24] Haoye Chai, Supeng Leng, Yijin Chen, and Ke Zhang. A hierarchical blockchain-enabled federated learning algorithm for knowledge sharing in internet of vehicles. *IEEE Transactions on Intelligent Transportation Systems*, 2020.
- [25] Shiva Raj Pokhrel and Jinho Choi. Federated learning with blockchain for autonomous vehicles: Analysis and design challenges. *IEEE Transactions on Communications*, 68(8):4734–4746, 2020.
- [26] Jiawen Kang, Zehui Xiong, Dusit Niyato, Yuze Zou, Yang Zhang, and Mohsen Guizani. Reliable federated learning for mobile networks. *IEEE Wireless Communications*, 27(2):72–80, 2020.
- [27] Jiawen Kang, Zehui Xiong, Xuandi Li, Yang Zhang, Dusit Niyato, Cyril Leung, and Chunyan Miao. Optimizing task assignment for reliable blockchain-empowered federated edge learning. *IEEE Transactions on Vehicular Technology*, 70(2):1910–1923, 2021.
- [28] Jiawen Kang, Zehui Xiong, Chunxiao Jiang, Yi Liu, Song Guo, Yang Zhang, Dusit Niyato, Cyril Leung, and Chunyan Miao. Scalable and communication-efficient decentralized federated edge learning with multi-blockchain framework. In *International Conference on Blockchain and Trustworthy Systems*, pages 152–165. Springer, 2020.
- [29] Wei Yang Bryan Lim, Jianqiang Huang, Zehui Xiong, Jiawen Kang, Dusit Niyato, Xian-Sheng Hua, Cyril Leung, and Chunyan Miao. Towards federated learning in uav-enabled internet of vehicles: A multi-dimensional contract-matching approach. *IEEE Transactions on Intelligent Transportation Systems*, 2021.
- [30] Jin-Hua Chen, Min-Rong Chen, Guo-Qiang Zeng, and Jia-Si Weng. Bdfi: A byzantine-fault-tolerance decentralized federated learning method for autonomous vehicle. *IEEE Transactions on Vehicular Technology*, 70(9):8639–8652, 2021.
- [31] Hong Liu, Shuaipeng Zhang, Pengfei Zhang, Xinqiang Zhou, Xuebin Shao, Geguang Pu, and Yan Zhang. Blockchain and federated learning for collaborative intrusion detection in vehicular edge computing. *IEEE Transactions on Vehicular Technology*, 2021.
- [32] Takayuki Nishio and Ryo Yonetani. Client selection for federated learning with heterogeneous resources in mobile edge. In *ICC 2019-2019 IEEE International Conference on Communications (ICC)*, pages 1–7. IEEE, 2019.
- [33] Latif U Khan, Shashi Raj Pandey, Nguyen H Tran, Walid Saad, Zhu Han, Minh NH Nguyen, and Choong Seon Hong. Federated learning for edge networks: Resource optimization and incentive mechanism. *IEEE Communications Magazine*, 58(10):88–93, 2020.
- [34] Youyang Qu, Longxiang Gao, Tom H Luan, Yong Xiang, Shui Yu, Bai Li, and Gavin Zheng. Decentralized privacy using blockchain-enabled federated learning in fog computing. *IEEE Internet of Things Journal*, 7(6):5171–5183, 2020.
- [35] Chenhao Xu, Yong Li, Yao Deng, Jiaqi Ge, Longxiang Gao, Mengshi Zhang, Yong Xiang, and Xi Zheng. ScEI: A smart-contract driven edge intelligence framework for iot systems. *arXiv preprint arXiv:2103.07050*, 2021.
- [36] Zeyad Al-Odat, Assad Abbas, and Samee U Khan. Randomness analyses of the secure hash algorithms, sha-1, sha-2 and modified sha. In *2019 International Conference on Frontiers of Information Technology (FIT)*, pages 316–3165. IEEE, 2019.
- [37] Roberto Doriguzzi-Corin, Stuart Millar, Sandra Scott-Hayward, Jesus Martinez-del Rincon, and Domenico Siracusa. Lucid: A practical, lightweight deep learning solution for ddos attack detection. *IEEE Transactions on Network and Service Management*, 17(2):876–889, 2020.
- [38] Sebastian Henningsen, Martin Florian, Sebastian Rust, and Björn Scheuermann. Mapping the interplanetary filesystem. In *2020 IFIP Networking Conference (Networking)*, pages 289–297. IEEE, 2020.
- [39] Hyesung Kim, Jihong Park, Mehdi Bennis, and Seong-Lyun Kim. Blockchain-enabled on-device federated learning. *IEEE Communications Letters*, 24(6):1279–1283, 2019.
- [40] Mansoor Shafi, Andreas F Molisch, Peter J Smith, Thomas Haustein, Peiyong Zhu, Prasan De Silva, Fredrik Tufvesson, Anass Benjebbour, and Gerhard Wunder. 5g: A tutorial overview of standards, trials, challenges, deployment, and practice. *IEEE journal on selected areas in communications*, 35(6):1201–1221, 2017.
- [41] Elli Androulaki, Artem Barger, Vita Bortnikov, Christian Cachin, Konstantinos Christidis, Angelo De Caro, David Enyeart, Christopher Ferris, Gennady Laventman, Yacov Manevich, et al. Hyperledger fabric: a distributed operating system for permissioned blockchains. In *Proceedings of the thirteenth EuroSys conference*, pages 1–15, 2018.
- [42] Han Xiao, Kashif Rasul, and Roland Vollgraf. Fashion-mnist: a novel image dataset for benchmarking machine learning algorithms. *arXiv preprint arXiv:1708.07747*, 2017.
- [43] Zhiyong Cui, Kristian Henrickson, Ruimin Ke, and Yin Hai Wang. Traffic graph convolutional recurrent neural network: A deep learning framework for network-scale traffic learning and forecasting. *IEEE Transactions on Intelligent Transportation Systems*, 2019.



Chenhao Xu received a BS degree in Software Engineering in 2018 from Beijing Institute of Technology, China. He is currently pursuing a Ph.D. degree at the School of Information Technology, Deakin University. His research interests include blockchain, federated learning, and IoT.



Globecom.

Youyang Qu received his B.S. degree of Mechanical Automation in 2002 and M.S. degree of Software Engineering in 2015 from Beijing Institute of Technology, respectively. He received his Ph.D. degree at School of Information Technology, Deakin University in 2019. His research interests focus on dealing with security and customizable privacy issues in Blockchain, Social Networks, Machine Learning, and IoT. He is active in communication society and has served as a TPC Member for IEEE flagship conferences including IEEE ICC and IEEE



Tom H. Luan received the B.Eng. degree from Xi'an Jiao Tong University, China, in 2004, the M.Phil. degree from The Hong Kong University of Science and Technology in 2007, and the Ph.D. degree from the University of Waterloo, Waterloo, ON, Canada, in 2012. He is currently a Professor with the School of Cyber Engineering, Xidian University, Xi'an, China. He has authored/co-authored more than 40 journal papers and 30 technical papers in conference proceedings, and has received one U.S. patent. His research mainly focuses on content distribution and media streaming in vehicular ad hoc networks and peer-to-peer networking, and the protocol design and performance evaluation of wireless cloud computing and edge computing.



Peter W. Eklund is Professor of AI and Machine Learning at Deakin University's School of Information Technology. Peter received his PhD from Linköping University in Sweden, has an M.Phil from Brighton University in the UK and was a graduate in Mathematics from the University of Wollongong. Peter has over 150 publications and is an elected fellow of the Australian Computer Society.



Yong Xiang received his B.E. and M.E. degrees from the University of Electronic Science and Technology of China, China, and PhD degree from The University of Melbourne, Australia. He is a Professor at the School of Information Technology, Deakin University, Australia. He is also the Associate Head of School (Research) and the Director of the Artificial Intelligence and Data Analytics Research Cluster. He has obtained a number of research grants (including several ARC Discovery and Linkage grants from the Australian Research

Council) and published numerous research papers in high-quality international journals and conferences. He is the coinventor of two U.S. patents and some of his research results have been commercialised. Dr Xiang is the Editor/Guest Editor of several international journals. He has been invited to give keynote speeches and chair committees in a number of international conferences, review papers for many international journals and conferences, serve on conference program committees, and chair technical sessions in conferences. Dr. Xiang is a senior member of the IEEE.



Longxiang Gao (SM17) received his PhD in Computer Science from Deakin University, Australia. He is currently a Professor at Qilu University of Technology (Shandong Academy of Sciences) and Shandong Computer Science Center (National Supercomputer Center in Jinan). He was a Senior Lecturer at School of Information Technology, Deakin University and a post-doctoral research fellow at IBM Research & Development, Australia. His research interests include Fog/Edge computing, Blockchain, data analysis and privacy protection.

Dr. Gao has over 90 publications, including patent, monograph, book chapter, journal and conference papers. Some of his publications have been published in the top venue, such as IEEE TMC, IEEE TPDS, IEEE IoTJ, IEEE TDSC, IEEE TVT, IEEE TCSS, IEEE TII and IEEE TNSE. He has been Chief Investigator (CI) for more than 20 research projects (the total awarded amount is over \$5 million), from pure research project to contracted industry research. He is a Senior Member of IEEE.